Ultrasound Obstet Gynecol 2013; **42**: 268–284
Published online in Wiley Online Library (wileyonlinelibrary.com). **DOI:** 10.1002/uog.12563

Fetal Intelligent Navigation Echocardiography (FINE): a novel method for rapid, simple, and automatic examination of the fetal heart

LAMI YEO*†‡ and ROBERTO ROMERO*‡

**Perinatology Research Branch, NICHD/NIH/DHHS, Bethesda, MD, USA and Detroit, MI, USA; †Department of Obstetrics and Gynecology, Wayne State University, Detroit, MI, USA; ‡Detroit Medical Center, Hutzel Women's Hospital, Detroit, MI, USA*

KEYWORDS: 4D; cardiac; congenital heart disease; fetal heart; prenatal diagnosis; spatiotemporal image correlation; STIC; ultrasound; Virtual Intelligent Sonographer Assistance; VIS-Assistance®

ABSTRACT

Objective *To describe a novel method (Fetal Intelligent Navigation Echocardiography (FINE)) for visualization of standard fetal echocardiography views from volume datasets obtained with spatiotemporal image correlation (STIC) and application of 'intelligent navigation' technology.*

Methods *We developed a method to: 1) demonstrate nine cardiac diagnostic planes; and 2) spontaneously navigate the anatomy surrounding each of the nine cardiac diagnostic planes (Virtual Intelligent Sonographer Assistance (VIS-Assistance®)). The method consists of marking seven anatomical structures of the fetal heart. The following echocardiography views are then automatically generated: 1) four chamber; 2) five chamber; 3) left ventricular outflow tract; 4) short-axis view of great vessels/right ventricular outflow tract; 5) three vessels and trachea; 6) abdomen/stomach; 7) ductal arch; 8) aortic arch; and 9) superior and inferior vena cava. The FINE method was tested in a separate set of 50 STIC volumes of normal hearts (18.6–37.2 weeks of gestation), and visualization rates for fetal echocardiography views using diagnostic planes and/or VIS-Assistance® were calculated. To examine the feasibility of identifying abnormal cardiac anatomy, we tested the method in four cases with proven congenital heart defects (coarctation of aorta, tetralogy of Fallot, transposition of great vessels and pulmonary atresia with intact ventricular septum).*

Results *In normal cases, the FINE method was able to generate nine fetal echocardiography views using: 1) diagnostic planes in 78–100% of cases; 2) VIS-Assistance® in 98–100% of cases; and 3) a combination of diagnostic planes and/or VIS-Assistance® in 98–100% of cases. In all four abnormal cases, the FINE method demonstrated evidence of abnormal fetal cardiac anatomy.*

Conclusions *The FINE method can be used to visualize nine standard fetal echocardiography views in normal hearts by applying 'intelligent navigation' technology to STIC volume datasets. This method can simplify examination of the fetal heart and reduce operator dependency. The observation of abnormal echocardiography views in the diagnostic planes and/or VIS-Assistance® should raise the index of suspicion for congenital heart disease. Published 2013. This article is a U.S. Government work and is in the public domain in the USA.*

INTRODUCTION

Congenital heart disease is the leading organ-specific birth defect[1], and is also the leading cause of infant mortality from congenital malformations[2]. More than half of infants affected with congenital heart disease are born to mothers without any previously known risk factors[3], and hence this provides the impetus to perform a comprehensive screening examination of the fetal heart in all pregnancies[4–6]. Yet, the prenatal diagnosis of congenital heart disease remains a challenge, as the sensitivity of ultrasound has ranged from 15 to 39%[2,7–14]. Some investigators have reported no secular improvement in sensitivity over a 10-year period[11]. Indeed, despite almost universal access to sonographic screening during pregnancy, only 28% of major congenital heart defects have been detected prenatally[10]. The lack of prenatal identification of congenital heart defects can have adverse consequences for the neonate[2,15–17]. The prenatal diagnosis of specific cardiac anomalies improves the preoperative

Correspondence to: Dr L. Yeo and Dr R. Romero, Perinatology Research Branch, NICHD, NIH, DHHS, Hutzel Women's Hospital, 3990 John R, Box 4, Detroit, MI 48201, USA (e-mail: lyeo@med.wayne.edu and romeror@mail.nih.gov)

Accepted: 13 February 2013

condition[18–22], neurologic outcome[23], and survival after surgery[17,20,24,25].

The difficulties in prenatal diagnosis are generally attributed to the complex anatomy of the heart, its motion, and small size. Adequate examination of the fetal heart depends on fetal position, is time consuming[26] and expertise and skill are required[27–29]. Therefore, the examination frequently does not include all the standard recommended cardiac views (e.g. four chamber, left and right ventricular outflow tracts, three vessels and trachea (3VT))[30–35].

A growing body of evidence suggests that three-dimensional (3D) sonography[36–48] and four-dimensional (4D) sonography with spatiotemporal image correlation (STIC) facilitate examination of the fetal heart[49–63], and may also be used to evaluate fetal cardiac function[64–67] and congenital heart disease[68–83]. STIC technology allows the acquisition of a volume dataset from the fetal heart and displays a cine loop of a complete single cardiac cycle in motion. However, extracting and displaying the recommended diagnostic planes from a volume dataset that can be dissected in many ways (i.e. planes) requires an in-depth knowledge of anatomy, and is difficult, operator-dependent, and time consuming. Planes and cardiac structures may be difficult to recognize, particularly when the anatomy is abnormal. Therefore, we and others have developed algorithms based upon STIC to assist users in systematically and efficiently interrogating volume datasets to allow the display of cardiac diagnostic planes[84–90]. Such algorithms were aimed at reducing operator dependency. Automated retrieval of cardiac diagnostic planes has also been reported using software applied to 3D static volumes of the fetal chest[91].

We describe herein a novel method (Fetal Intelligent Navigation Echocardiography (FINE)) to interrogate a STIC volume dataset using 'intelligent navigation', which allows the automatic display of nine standard fetal echocardiography views[92] required to diagnose most cardiac defects. The potential value of the FINE method is also illustrated in four cases with congenital heart defects.

METHOD

Intelligent navigation

We propose the term 'intelligent navigation' (described elsewhere)[93] to refer to a new method of interrogation of a volume dataset in which identification and selection of key anatomical landmarks can: 1) generate a geometrical reconstruction of the organ of interest; and 2) automatically navigate, find, extract, and display specific diagnostic planes. This can be accomplished using operator-independent algorithms, which are both predictable and adaptive. Intelligent navigation includes the following: 1) marking of anatomical structures in the volume dataset; 2) display of *diagnostic planes*; and 3) operator-independent sonographic navigation and exploration of the surrounding structures in previously identified diagnostic planes, using *Virtual Intelligent Sonographer Assistance* (*VIS-Assistance*®)[93].

Development phase of Fetal Intelligent Navigation Echocardiography

The development of the FINE method was based on STIC volume datasets obtained from patients examined at the Detroit Medical Center/Wayne State University and at the Perinatology Research Branch, NICHD, NIH, DHHS. All women had been enrolled in research protocols approved by the Institutional Review Board of the NICHD, NIH, and by the Human Investigation Committee of Wayne State University. All participants provided written informed consent for the use of ultrasound images for research purposes.

Using STIC technology (Voluson E8 Expert; GE Healthcare, Milwaukee, WI, USA), 4D volume datasets of the fetal heart were acquired from an apical four-chamber view using hybrid mechanical and curved array transducers (2–5 or 4–8 MHz) by transverse sweeps through the fetal chest in patients examined in our unit. Acquisition times ranged from 7.5 to 12.5 seconds, depending on fetal motion, and the angle of acquisition ranged between 20 and 45°, depending on gestational age. Fifty-one volume datasets of normal hearts (19.5–39.3 weeks of gestation) were selected by the investigators. The criteria for inclusion were: 1) fetal spine located between the 5- and 7-o'clock positions (reducing the possibility of shadowing from the ribs or spine); and 2) upper mediastinum and stomach contained within the volume. Five (9.8%) fetuses were in breech presentation so that the cardiac apex was originally pointing to the right side of the screen. All 51 STIC datasets were used to develop and refine the FINE method in the initial phase of work.

A software system that is specifically designed for volumetric analysis and rendering was used to analyze the STIC datasets (SONOCUBIC® Classic Blue Series; Medge Platforms Inc., New York, NY, USA). This system was chosen because it possesses a suite of tools that was considered suitable for the evaluation of STIC volumes. For example, the technology is capable of independently tilting tomographic slices in a non-parallel fashion in order to display certain anatomical structures. This was considered important for the great vessels, which may not be shown appropriately when dissection occurs parallel to the four-chamber view. STIC datasets were stored in ViewPoint (GE Healthcare) and DICOM files were then imported into the SONOCUBIC® software system. The system was installed on a Dell Inspiron XPS M1710 laptop computer (Dell Inc., Round Rock, TX, USA), using the operating system Microsoft Windows XP, Media Center Edition, Version 2002, Service Pack 3 (Microsoft Corp., Redmond, WA, USA). It is noteworthy that it is also possible to import STIC volumes in real-time. Once a STIC volume dataset has been acquired during the course of an ultrasound examination, it can be sent to a computer (in which the SONOCUBIC® software system has been installed) where the volume will

automatically be converted into a two-dimensional (2D) cine loop available for assessment (see the section below on *STICLoop*™).

Development of the FINE method first involved evaluation of different anatomical landmarks regarding their potential to generate a geometrical model of the fetal heart, which could be dissected to display standard echocardiography views. Structures that were considered included: the apex of the heart, atrioventricular valves, crux, atrial walls, ventricular septum, aorta, pulmonary artery, superior and inferior vena cava, etc. Next, we determined the minimum number (parsimonious) of anatomical landmarks required to produce a geometrical model of the fetal heart from which the echocardiography views could be extracted. Selection of landmarks took into account the need to reduce operator error, and also took advantage of the system's ability to recognize the cardiac phase, which can facilitate marking (e.g. closed pulmonary valve). Anatomical landmarks that could easily be identified by sonologists were preferred. For example, we favored structures observed at the level of the four-chamber view of the heart (such as the crux) because this is the most easily[94] and commonly obtained plane in fetal echocardiography. Additional landmarks were required as it became clear that adequate modeling of the fetal heart could not be achieved without including landmarks outside the four-chamber view. We selected further potential landmarks based upon their potential to add more information to construct a geometrical model of the fetal heart, and the empirical evidence that this indeed was the case. Repeated iterations were performed to select informative landmarks, and a large number were discarded because they were neither informative nor reliable.

After marking seven anatomical structures of the heart, we employed the feature Anatomic Box® to perform the calculations required to reconstruct the heart in three dimensions and generate the standard *fetal echocardiography views* that had been prespecified before the onset of the project. Nine views were considered desirable: 1) four chamber; 2) five chamber; 3) left ventricular outflow tract; 4) short-axis view of great vessels/right ventricular outflow tract; 5) 3VT; 6) abdomen/stomach; 7) ductal arch; 8) aortic arch; and 9) superior and inferior vena cava. Diagnostic planes are displayed approximately 3 seconds after marking is completed.

One of the goals of this effort was to enable automatic realignment of STIC volumes, and the reorientation and standardization of the anatomical position, so that the fetus and diagnostic planes are consistently displayed in the same manner every time, regardless of the fetal position or initial orientation (e.g. converts a true breech to a 'vertex' presentation, places the spine at 6 o'clock)[93]. This was considered important so that marking anatomical structures would be easier, as each would be expected to be in the same location on the screen. Moreover, structures and fetal anatomy would be more easily recognizable by the user. Therefore, we designed the FINE method so that the orientation of fetal images would be standardized for: 1) axial images (fetal left on the left side of the screen, and fetal right on the right side of the screen; the cardiac apex would always point to the upper left corner of the screen); and 2) longitudinal images (cranial end on the left side of the screen, and caudal end on the right side of the screen).

Another objective of the study was to explore the feasibility of automatic labeling of the nine fetal echocardiography views (i.e. diagnostic planes), left and right side of the fetus, cranial and caudal ends, as well as the atrial chambers, ventricular chambers, great vessels (aorta and pulmonary artery), superior and inferior vena cava, and stomach.

Virtual Intelligent Sonographer Assistance

We recognized that the nine fetal echocardiography views represent a recommendation of professional organizations to simplify and standardize examination of the fetal heart. However, the complex anatomy of the fetal heart and anatomical variations may require additional interrogation of a given diagnostic plane. To accomplish this, we developed a novel tool coined *Virtual Intelligent Sonographer Assistance (VIS-Assistance®)*, which is operator-independent[93]. This tool allows sonographic navigation and exploration of the surrounding structures in each of the nine cardiac diagnostic planes (e.g. four-chamber view). VIS-Assistance® 'scans' the volume in a purposeful and targeted manner (in the form of a videoclip) with the goal of visualizing specific structures. These navigational movements are intelligent owing to the design of pivot points which change, and around which there are sequential movements. The maximum duration of VIS-Assistance® for each echocardiography view was: 1) four chamber (1 min 26 seconds); 2) five chamber (3 min 30 seconds); 3) left ventricular outflow tract (1 min 40 seconds); 4) short-axis view of great vessels/right ventricular outflow tract (2 min 36 seconds); 5) 3VT (1 min 6 seconds); 6) abdomen/stomach (32 seconds); 7) ductal arch (1 min 57 seconds); 8) aortic arch (1 min 4 seconds); and 9) superior and inferior vena cava (1 min 36 seconds). The time duration to observe all nine VIS-Assistance® videoclips is 15 min 27 seconds. Therefore, VIS-Assistance®: 1) improves the success of obtaining the fetal echocardiography view of interest; and 2) provides more information about the diagnostic plane and its surrounding structures[93].

In four cardiac VIS-Assistance® views (3VT, left ventricular outflow tract, short-axis view of great vessels/right ventricular outflow tract and abdomen/stomach) we prespecified that certain anatomical structures should also be visualized in order to consider the VIS-Assistance® as being successful in depicting the echocardiography view, as follows: 1) 3VT: three-vessel view, pulmonary valve and transverse aortic arch view[95]; 2) left ventricular outflow tract: mitral valve, aortic valve and ventricular septum; 3) short-axis view of great vessels/right ventricular outflow tract: pulmonary valve and tricuspid valve; and 4) abdomen/stomach: stomach and four-chamber view (to determine situs). Moreover, for the four-chamber view

VIS-Assistance®, we recorded how often the atrial septum (both septum primum and septum secundum) and pulmonary veins could be visualized when compared with the four-chamber view diagnostic plane.

The FINE method includes the display of nine cardiac diagnostic planes and VIS-Assistance®, and was developed after examining and testing the 51 STIC volumes repeatedly. Each round of testing involved the examination of 459 diagnostic planes (51 STIC volumes × 9) and 459 VIS-Assistance® videoclips (51 STIC volumes × 9), for a total of 918 images. Once the final version of the FINE method had been established (in the development phase), visualization rates for the nine fetal echocardiography views using diagnostic planes and/or VIS-Assistance® were calculated based on the 51 STIC volumes. When necessary, adequacy of a given echocardiography view was determined by comparison with the 'gold standard' (view obtained by expert manual navigation of the STIC volume using 4D View (GE Healthcare)).

Testing phase of Fetal Intelligent Navigation Echocardiography

STICLoop™

Once the development phase was complete, we tested the FINE method in a new set of 50 STIC volume datasets from patients previously examined in our unit and diagnosed to have a normal fetal heart. Each STIC volume was first evaluated to determine its appropriateness before the FINE method was applied. To accomplish this, we developed the *STICLoop*™. Once a STIC volume is loaded into the software system, it is converted into a 2D cine loop that automatically scrolls in a continuous fashion. With STICLoop™, the image on the screen begins with the initial frame that was obtained by the mechanical probe, and automatic scrolling through all the frames occurs until the last frame acquired in the sweep is reached. We used a cine rate of 8–12 loops/min to evaluate the STIC volumes.

The STICLoop™ (2D cine loop) was developed to facilitate detection of: 1) discontinuity or undulating movements that could modify anatomical structure representation and are due to motion artifacts or errors in STIC assembly; 2) azimuthal issues (tilted acquisitions); and 3) 'drifting spines', in which the spine location 'migrates' on the screen. We prefer to use STICLoop™ as an aid to determine the appropriateness of STIC volumes, rather than manual navigation through multiplanar views. The benefit of observing a 2D cine loop is that it allows improved detection of problems (e.g. undulating movements) because it runs automatically at a constant speed and is also operator-independent (Videoclips S1–S3). This is in contrast to manual navigation through multiplanar views, in which problems may be hidden or underestimated due to speed variability generated when a user operates the mouse. For example, if a fetus has moved quickly during the STIC acquisition, a few frames could be displaced from the rest. Yet, this may not be as noticeable when manually navigating through multiplanar views, and may be more likely to be detected using STICLoop™.

In order to determine whether STIC volumes were appropriate, all of the following criteria needed to be met using STICLoop™: 1) fetal spine located between the 5- and 7-o'clock positions (reducing the possibility of shadowing from the ribs or spine); 2) minimal or no motion artifacts observed (smooth sweep without evidence of abrupt jumps or discontinuous movements); 3) inclusion of upper mediastinum as well as stomach within the volume; 4) minimal or absent shadowing (which could obscure visualization of cardiac anatomy); 5) adequate image quality; 6) sequential axial planes parallel to each other, similar to a loaf of bread (i.e. no 'drifting spine'); and 7) no azimuthal issues observed (i.e. atria/ventricles do not appear foreshortened in the four-chamber view). Moreover, we also considered STIC volumes to be appropriate (using 4D view) if: 1) they contained the actual echocardiography view (e.g. left ventricular outflow tract); and 2) minimal or no motion artifacts were observed in the sagittal plane (after pressing the Initiate 'All' button, 50% speed in Auto Cine).

Testing of the FINE method

Next, we tested the FINE method in a new set of 50 STIC volume datasets of normal hearts. Testing consisted of evaluating 450 diagnostic planes (50 STIC volumes × 9) and 450 VIS-Assistance® videoclips (50 STIC volumes × 9), for a total of 900 images. Therefore, for testing purposes, the time taken to analyze each STIC volume dataset was, at most, approximately 30 min because each diagnostic plane and VIS-Assistance® videoclip was evaluated. Volume datasets in this phase were obtained from fetuses between 18.6 and 37.2 weeks of gestation. Ten (20%) fetuses were in a breech presentation. Visualization rates for the nine fetal echocardiography views using diagnostic planes and/or VIS-Assistance® were calculated. When necessary, adequacy of a given echocardiography view was determined by comparison with the 'gold standard' (view obtained by expert manual navigation of the STIC volume using 4D View).

For each STIC volume dataset ($n = 50$) we also calculated: 1) the maximum number of fetal echocardiography views that were successfully obtained through diagnostic planes or VIS-Assistance®; and 2) the success rate of obtaining four specific fetal echocardiography views (four chamber; left ventricular outflow tract; short-axis view of great vessels/right ventricular outflow tract; and abdomen/stomach) through diagnostic planes or VIS-Assistance®.

Finally, we tested the FINE method in four fetuses with congenital heart defects (confirmed by postnatal echocardiography) to determine whether abnormal cardiac anatomy could be identified. The cases consisted of: coarctation of the aorta (25 weeks of gestation), tetralogy of Fallot (25 weeks of gestation), transposition of the great vessels (28 weeks of gestation) and pulmonary atresia with intact ventricular septum (29 weeks of gestation).

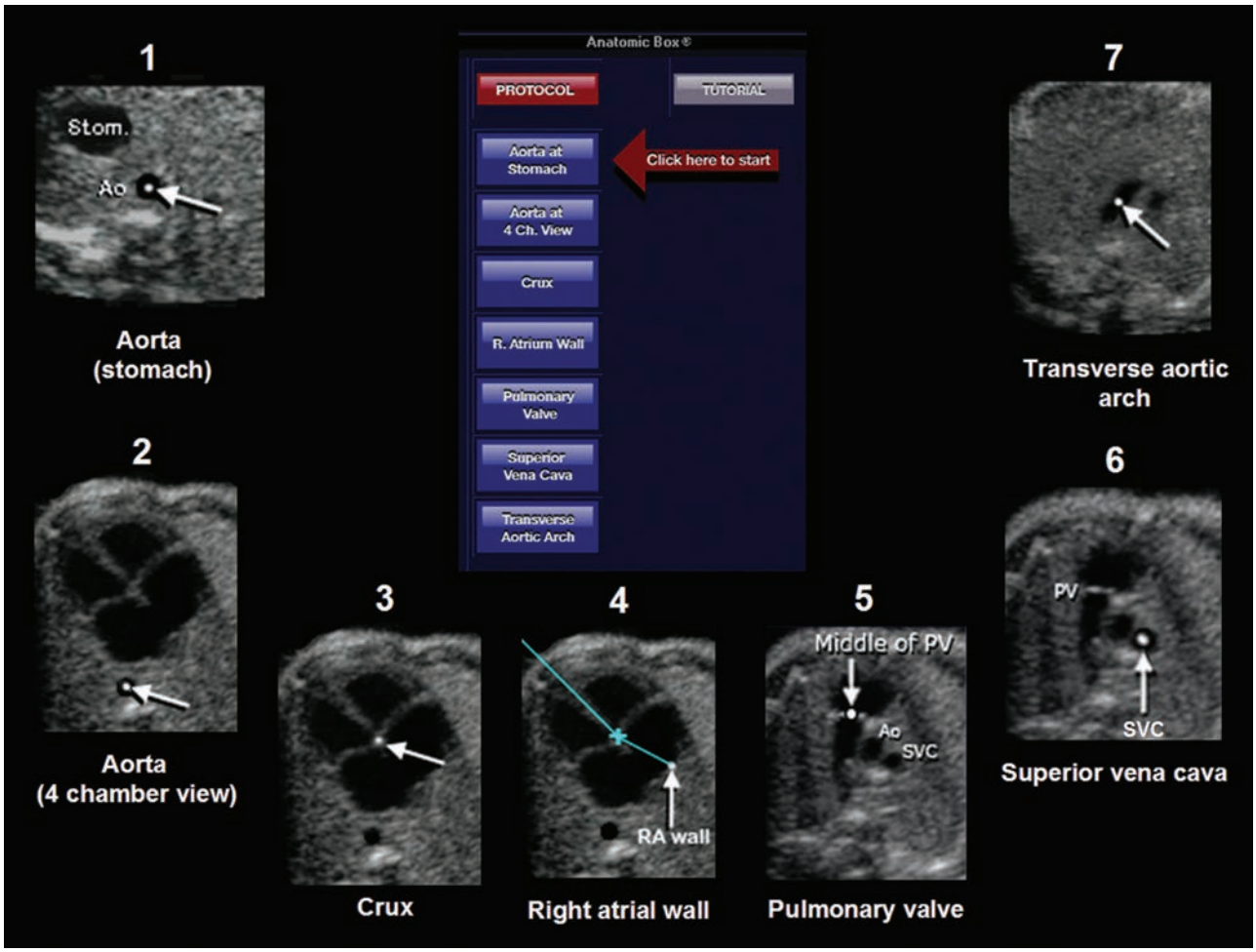

Figure 1 Seven anatomical structures within the heart that are marked using Anatomic Box® (also see Videoclip S4): 1) cross-section of the aorta at the level of the stomach; 2) cross-section of the aorta at the level of the four-chamber view; 3) crux; 4) right atrial wall; 5) pulmonary valve; 6) cross-section of the superior vena cava; and 7) transverse aortic arch. Ao, aorta; PV, pulmonary valve; R., right; RA, right atrium; Stom., stomach; SVC, superior vena cava.

RESULTS

The seven anatomical structures of the heart (Figure 1 and Videoclip S4) chosen for marking in Anatomic Box® were (in order): 1) cross-section of the aorta at the level of the stomach; 2) cross-section of the aorta at the level of the four-chamber view; 3) crux; 4) right atrial wall; 5) pulmonary valve; 6) cross-section of the superior vena cava; and 7) transverse aortic arch.

Visualization rates for fetal echocardiography views in normal fetuses (development and testing phases)

In the *development phase* (51 STIC volumes), the final version of the FINE method was able to generate nine fetal echocardiography views using: 1) diagnostic planes in 73–100% of cases; 2) VIS-Assistance® in 98–100% of cases; and 3) a combination of diagnostic planes and/or VIS-Assistance® in 98–100% of cases (Table 1).

In the *testing phase* (50 STIC volumes), the FINE method was able to generate nine fetal echocardiography views using: 1) diagnostic planes in 78–100% of cases; 2) VIS-Assistance® in 98–100% of cases; and 3) a combination of diagnostic planes and/or VIS-Assistance® in 98–100% of cases (Table 2). Figure S1 shows an example of the nine cardiac diagnostic planes in a single template, and Figure 2 shows the same template but with the additional feature of automatic labeling through intelligent navigation. Videoclip S5 demonstrates the nine cardiac diagnostic planes both before and after activation of automatic labeling.

Table 3 displays the maximum number of fetal echocardiography views successfully obtained through diagnostic planes or VIS-Assistance® for each normal STIC volume dataset ($n = 50$). For diagnostic planes, 76% ($n = 38$) of STIC volumes demonstrated either eight (36%; $n = 18$) or all nine (40%; $n = 20$) echocardiography views, while 18% ($n = 9$) demonstrated seven views. For VIS-Assistance®, 94% ($n = 47$) of STIC volumes demonstrated all nine echocardiography views, while 6% ($n = 3$) demonstrated eight views.

For each normal STIC volume dataset ($n = 50$), the success rate of obtaining the four-chamber view, left ventricular outflow tract view, short-axis view of great vessels/right ventricular outflow tract and abdomen/stomach view was 74% ($n = 37$) using diagnostic planes and 96% ($n = 48$) using VIS-Assistance®.

Table 1 Development phase of Fetal Intelligent Navigation Echocardiography (FINE): success rates of obtaining nine fetal echocardiography views after applying intelligent navigation to 51 normal spatiotemporal image correlation (STIC) volume datasets using diagnostic planes and/or Virtual Intelligent Sonographer Assistance (VIS-Assistance®)

	Diagnostic plane alone (n = *51*)		*VIS-Assistance® alone* (n = *51*)		*Diagnostic plane and/or VIS-Assistance®* (n = *51*)	
Fetal echocardiography view	n *(%)*	*95% CI**	n *(%)*	*95% CI**	n *(%)*	*95% CI**
1. Four chamber	47 (92)	81 to 97	51 (100)	92 to 100	51 (100)	92 to 100
2. Five chamber	47 (92)	81 to 97	51 (100)	92 to 100	51 (100)	92 to 100
3. LVOT	45 (88)	76 to 95	51 (100)	92 to 100	51 (100)	92 to 100
4. Short-axis view of great vessels/RVOT	42 (82)	70 to 91	51 (100)	92 to 100	51 (100)	92 to 100
5. 3VT	44 (86)	74 to 94	50 (98)	89 to > 99.9	50 (98)	89 to > 99.9
6. Abdomen/stomach	51 (100)†	92 to 100	51 (100)‡	92 to 100	51 (100)	92 to 100
7. Ductal arch	37 (73)	59 to 83	51 (100)	92 to 100	51 (100)	92 to 100
8. Aortic arch	44 (86)	74 to 94	51 (100)	92 to 100	51 (100)	92 to 100
9. SVC/IVC	41 (80)	67 to 89	51 (100)	92 to 100	51 (100)	92 to 100
SVC	47 (92)	81 to 97	—	—	—	—
IVC	43 (84)	72 to 92	—	—	—	—

*The Wald method was used to calculate two-sided CIs for proportions expressed in the table; as the true proportion cannot exceed 100%, upper confidence limits are truncated at 100%. †Defined as visualization of the stomach in the diagnostic plane. ‡Defined as visualization of both the stomach and four-chamber view in VIS-Assistance® (to determine situs). 3VT, three-vessels and trachea; IVC, inferior vena cava; LVOT, left ventricular outflow tract; RVOT, right ventricular outflow tract; SVC, superior vena cava.

Table 2 Testing phase of Fetal Intelligent Navigation Echocardiography (FINE): success rates of obtaining nine fetal echocardiography views after applying intelligent navigation to 50 normal spatiotemporal image correlation (STIC) volume datasets using diagnostic planes and/or Virtual Intelligent Sonographer Assistance (VIS-Assistance®)

	Diagnostic plane alone (n = *50*)		*VIS-Assistance® alone* (n = *50*)		*Diagnostic plane and/or VIS-Assistance®* (n = *50*)	
Fetal echocardiography view	n *(%)*	*95% CI**	n *(%)*	*95% CI**	n *(%)*	*95% CI**
1. Four chamber	48 (96)	86 to 100	50 (100)	92 to 100	50 (100)	92 to 100
2. Five chamber	48 (96)	86 to 100	50 (100)	92 to 100	50 (100)	92 to 100
3. LVOT	45 (90)	78 to 96	49 (98)	89 to > 99.9	49 (98)	89 to > 99.9
4. Short-axis view of great vessels/RVOT	42 (84)	71 to 92	50 (100)	92 to 100	50 (100)	92 to 100
5. 3VT	46 (92)	81 to 97	50 (100)	92 to 100	50 (100)	92 to 100
6. Abdomen/stomach	50 (100)†	92 to 100	49 (98)‡	89 to > 99.9	50 (100)	92 to 100
7. Ductal arch	39 (78)	65 to 87	49 (98)	89 to > 99.9	49 (98)	89 to > 99.9
8. Aortic arch	45 (90)	78 to 96	50 (100)	92 to 100	50 (100)	92 to 100
9. SVC/IVC	41 (82)	69 to 90	50 (100)	92 to 100	50 (100)	92 to 100
SVC	46 (92)	81 to 97	—	—	—	—
IVC	43 (86)	74 to 93	—	—	—	—

*The Wald method was used to calculate two-sided CIs for proportions expressed in the table; as the true proportion cannot exceed 100%, upper confidence limits are truncated at 100%. †Defined as visualization of the stomach in the diagnostic plane. ‡Defined as visualization of both the stomach and four-chamber view in VIS-Assistance® (to determine situs). 3VT, three-vessels and trachea; IVC, inferior vena cava; LVOT, left ventricular outflow tract; RVOT, right ventricular outflow tract; SVC, superior vena cava.

Comments about diagnostic planes in normal fetuses

One of the anatomical structures to be marked in Anatomic Box® is the right atrial wall. This is accomplished by clicking on the crux and then placing the preconfigured line (which appears next) over the ventricular septum. The inferior portion of this line is angled toward the right atrial wall for subsequent marking by the user (Figure 1). However, to improve the success rate of obtaining the left ventricular outflow tract in the diagnostic plane, we also designed an alternative straight (*vs* angled) line to mark the atrial wall. In 30% ($n = 15$) of 50 cases, we employed the straight line. When using either line for marking the atrial wall, the left ventricular outflow tract diagnostic plane was successfully obtained in 90% ($n = 45$) of cases (Table 2). When using only the angled line to mark the right atrial wall, VIS-Assistance® was able to demonstrate the left ventricular outflow tract successfully in 98% ($n = 49$) of cases (Table 2).

Comments about VIS-Assistance® in normal fetuses

Figure 3 and Videoclip S6 show different examples in which the left ventricular outflow tract view was unsuccessfully or suboptimally obtained using the diagnostic plane; however, this view was successfully obtained using VIS-Assistance®.

One of the advantages of the four-chamber view VIS-Assistance® is that it enables visualization of the atrial septum (both septum primum and septum secundum) and pulmonary veins (Videoclip S7). Both the septum primum and septum secundum were seen in 46% ($n = 23$)

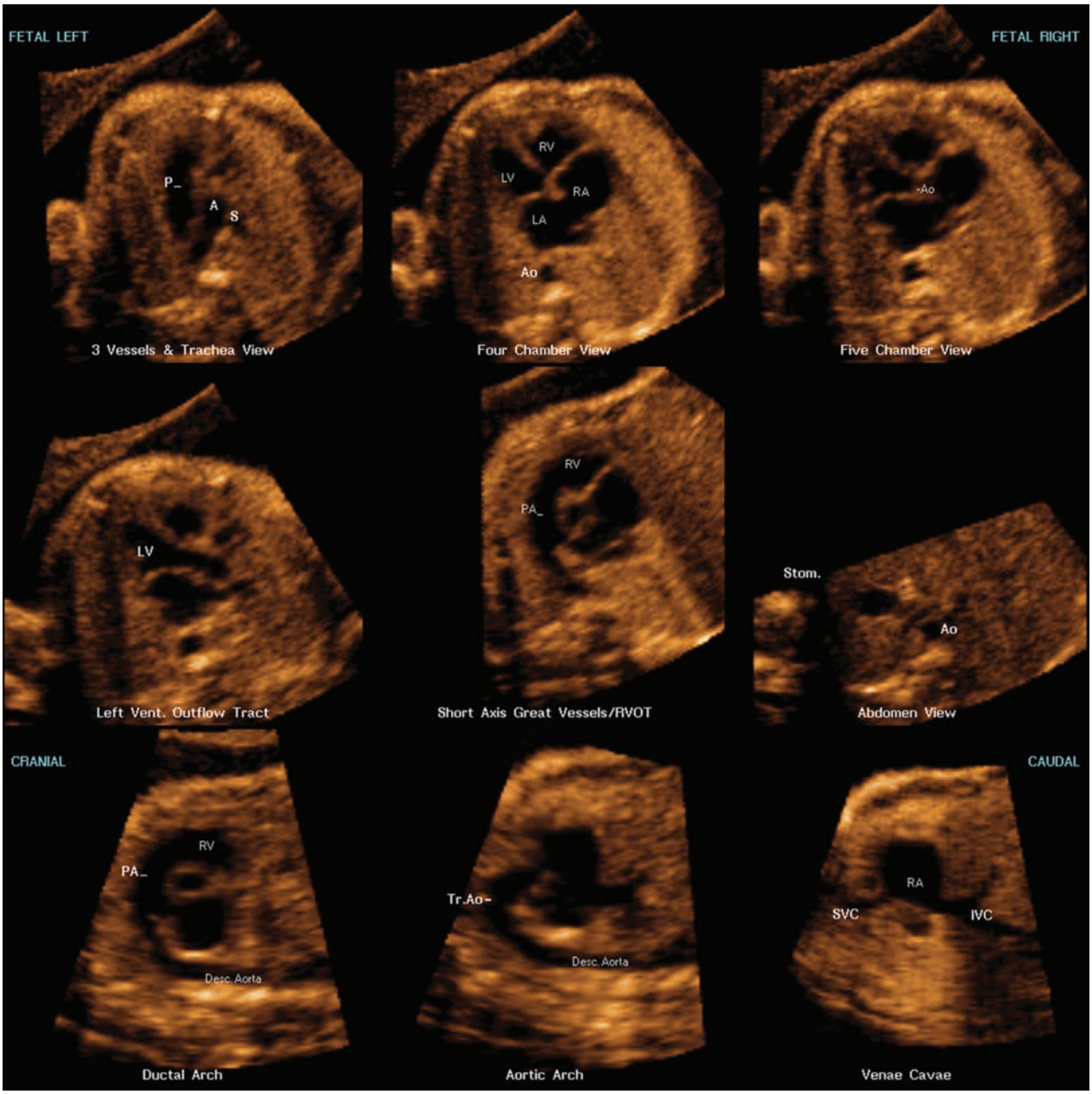

Figure 2 Nine cardiac diagnostic planes (same as Figure S1) with the unique feature of automatic labeling (through intelligent navigation) of each plane, anatomical structures, fetal left and right sides, and cranial and caudal ends (also see Videoclip S5). The labeling is distinctive because it stays with the corresponding anatomical structure(s), even as the image is increased in size (zoom). A, transverse aortic arch; Ao, aorta; Desc., descending; IVC, inferior vena cava; LA, left atrium; LV, left ventricle; P, pulmonary artery; PA, pulmonary artery; RA, right atrium; RV, right ventricle; RVOT, right ventricular outflow tract; S, superior vena cava; Stom., stomach; SVC, superior vena cava; Tr., transverse; Vent., ventricular.

of cases of the four-chamber view diagnostic plane, but were seen in 94% ($n = 47$) when VIS-Assistance® was employed. However, the five-chamber view diagnostic plane was able to demonstrate the septum secundum successfully in the three cases in which the four-chamber view VIS-Assistance® did not. The pulmonary veins were seen in 44% ($n = 22$) of cases of the four-chamber view diagnostic plane, but were seen in 96% ($n = 48$) of cases when VIS-Assistance® was employed. However, the five-chamber view VIS-Assistance® was able to demonstrate the pulmonary veins successfully in the two cases in which the four-chamber view VIS-Assistance® did not. For the abdomen/stomach VIS-Assistance®, both the stomach and the four-chamber view were visualized in 98% ($n = 49$) of cases, so that situs could be determined (Table 2).

An example of VIS-Assistance® in which the volume is 'scanned' spontaneously in a purposeful and targeted manner to visualize specific structures is illustrated in the 3VT view (Figure 4, Videoclip S8). While the 3VT view is demonstrated in the diagnostic plane, VIS-Assistance® also demonstrates the three-vessel view and transverse aortic arch views through navigational movements (Videoclip S8).

Table 3 Number of fetal echocardiography views successfully obtained through diagnostic planes or Virtual Intelligent Sonographer Assistance (VIS-Assistance®) for each normal spatiotemporal image correlation (STIC) volume dataset ($n = 50$)

Number of fetal echocardiography views successfully obtained for each normal STIC volume dataset (n = *9 maximum*)	*Diagnostic planes* (n = *50*)		*Virtual Intelligent Sonographer Assistance (VIS-Assistance®)* (n = *50*)	
	n	%	n	%
5	1	2	—	—
6	2	4	—	—
7	9	18	—	—
8	18	36	3	6
All nine views obtained	20	40	47	94
Total	50	100	50	100

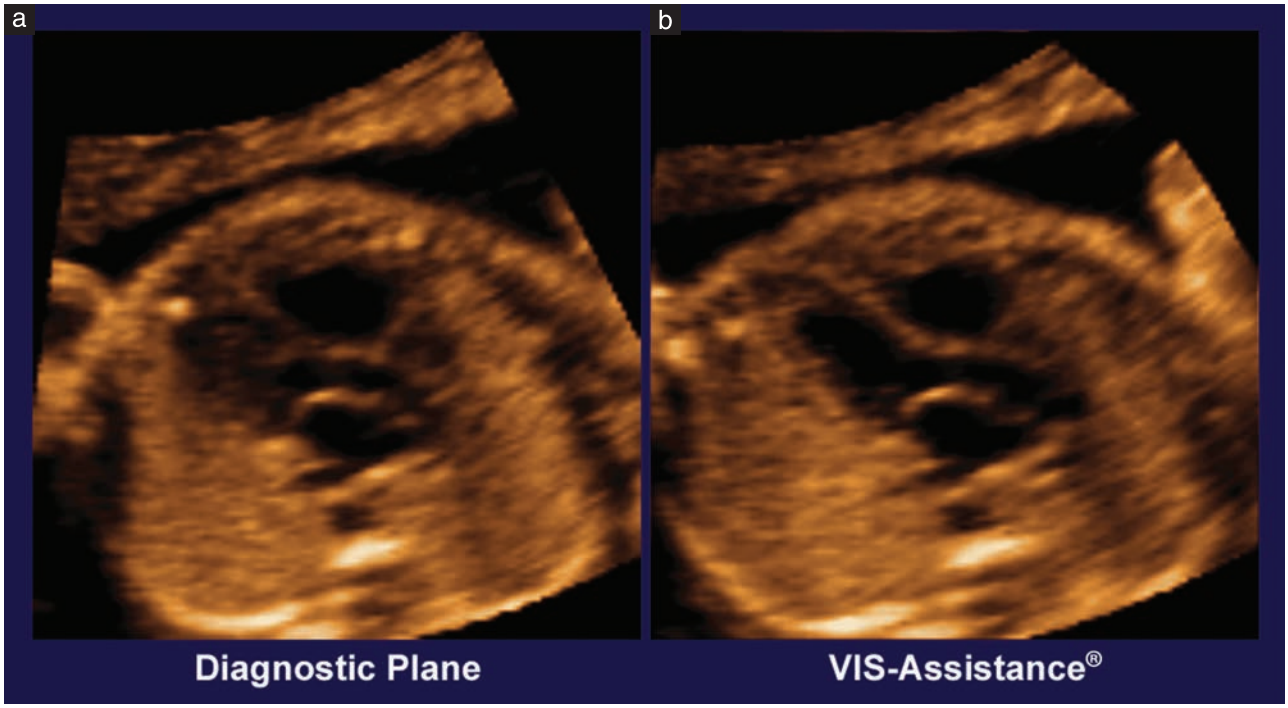

Figure 3 Left ventricular outflow tract view. This example shows that the left ventricular outflow tract was not successfully obtained using the diagnostic plane (a), but was successfully obtained (automatically) using Virtual Intelligent Sonographer Assistance (VIS-Assistance®) (b). Also see Videoclip S6.

Videoclip S9 shows a fetus in which the left ventricle appears foreshortened (five-chamber view diagnostic plane) and there is uncertainty as to whether this is due to a tilted plane (azimuth) or because the left ventricle is truly hypoplastic. By activating VIS-Assistance®, it is evident that the 'small' left ventricle is not hypoplastic, but rather is due to an azimuthal effect.

FINE method in four cases of congenital heart defects

Coarctation of aorta

The FINE method is illustrated in a fetus with coarctation of the aorta at 25 weeks of gestation (Figure 5, Videoclip S10). The 3VT view shows evidence of a narrow transverse aortic arch. In the four-chamber view, the left ventricle appears narrow compared to the right ventricle; however, it is apex-forming and there is normal movement of the mitral valve. The right side of the heart appears enlarged, and the right ventricle is moderately hypertrophied. The five-chamber view shows a ventricular septal defect and a narrow aortic root. The left ventricular outflow tract view also shows the ventricular septal defect, along with a narrow aorta. In the short-axis view of great vessels/right ventricular outflow tract, the cross-section of the aorta is small when compared to the pulmonary artery. The coarctation is demonstrated clearly in the aortic arch view.

Tetralogy of Fallot

In a fetus with tetralogy of Fallot at 25 weeks of gestation, six echocardiography views were abnormal and demonstrated the typical features of this condition (Figure S2, Videoclip S11). The 3VT view shows a narrow pulmonary artery caused by pulmonary stenosis. Not surprisingly, the four-chamber view appears normal in the diagnostic plane; however, VIS-Assistance® demonstrates a large

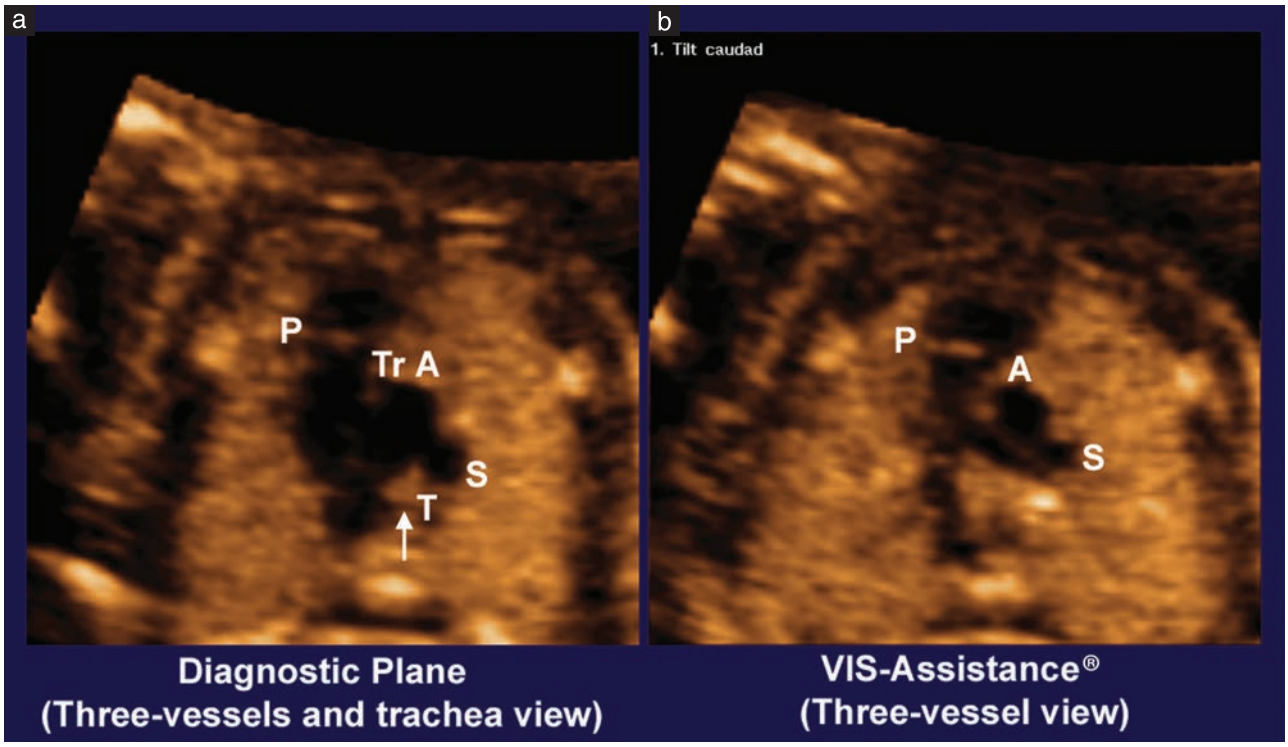

Figure 4 Three-vessels and trachea view successfully obtained in the diagnostic plane (a). Through Virtual Intelligent Sonographer Assistance (VIS-Assistance®), the three-vessel view is also demonstrated by automatic navigational movements (shown as '1. Tilt caudad') (b). In the three-vessel view, the pulmonary artery is seen to bifurcate into the ductus arteriosus and the right pulmonary artery. Labeling for both images was performed manually in this example. A, cross-section of aorta; P, pulmonary artery; T, trachea (shown by arrow); Tr A, transverse aortic arch; S, superior vena cava. Also see Videoclip S8.

ventricular septal defect. Both the five-chamber and left ventricular outflow tract views show an overriding aorta, dilated aortic root and ventricular septal defect. In the short-axis view of great vessels/right ventricular outflow tract, the pulmonary artery is narrow with a small ductus arteriosus, and the cross-sectional aorta is dilated. There is difficulty in visualizing a normal ductal arch in both the diagnostic plane and VIS-Assistance®.

Transposition of the great vessels

A case with transposition of the great vessels at 28 weeks of gestation provides an example in which anatomical structures for marking are technically not in their usual location and the anatomy appears atypical in the axial plane (STICLoop™). Specifically, marking what appears to be the 'pulmonary valve' is actually the true aortic valve, since the aorta arises anteriorly from the right ventricle. Moreover, in the axial plane in which marking the 'pulmonary valve' and the cross-section of the superior vena cava occurs, a third vessel in between these two structures (i.e. normally the aorta) is notably missing. Yet, it is noteworthy that owing to the design of the FINE method (i.e. specific anatomical structures chosen for marking and the system automatically scrolling through the volume to the level of the most likely location of such anatomical structures), the 'pulmonary valve' still 'appears' to be present and in its usual location for this case. In other words, despite the presence of true ventriculoarterial discordance, the anatomy was such that the process of *marking* anatomical structures did not appear to be different from the usual routine.

For this case, the FINE method demonstrated that five of the echocardiography views were abnormal, consistent with the diagnosis of transposition of the great vessels (Figure S3, Videoclip S12). In the 3VT view, only two vessels are seen (the aorta arising from the right ventricle and a cross-section of the superior vena cava). When VIS-Assistance® is activated, another vessel (the pulmonary artery) that is posterior and to the left of the aorta now becomes visible. The four-chamber view appears completely normal. For the five-chamber view, although the diagnostic plane appears normal, the great vessels arising parallel and side-by-side from the ventricles are visualized in VIS-Assistance®. The left ventricular outflow tract view appears abnormal because only the proximal portion of an outflow tract is seen arising from the left ventricle. VIS-Assistance® (Videoclip S13) further shows two great vessels arising parallel and side-by-side from the ventricles (the pulmonary artery from the left ventricle and the aorta from the right ventricle). There is difficulty in visualizing a normal short-axis view of great vessels/right ventricular outflow tract in both the diagnostic plane and VIS-Assistance®. For the ductal arch view, the diagnostic plane appears abnormal. VIS-Assistance® is able to demonstrate further the aorta arising anteriorly from the right ventricle, while

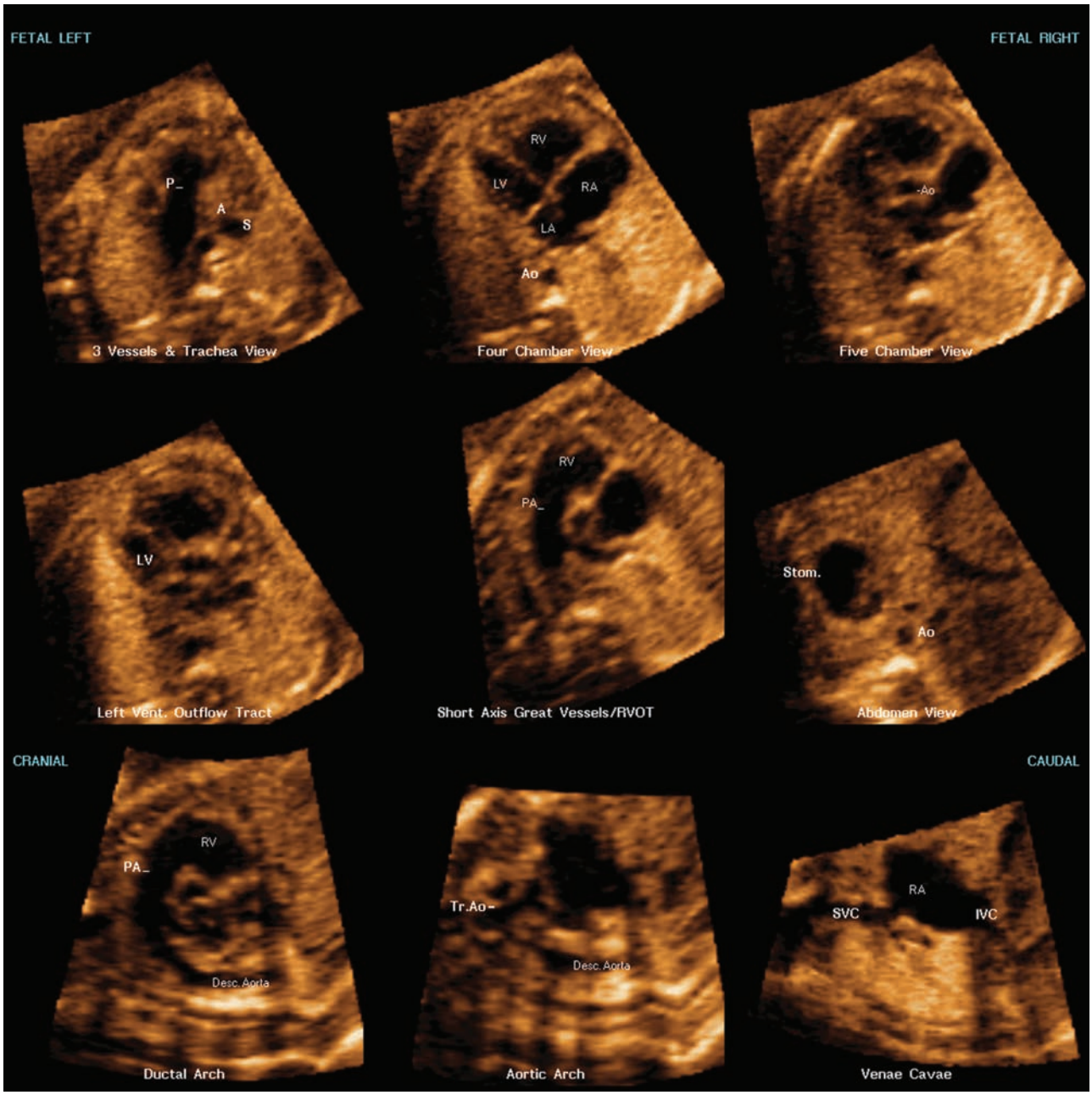

Figure 5 Application of the Fetal Intelligent Navigation Echocardiography (FINE) method to a fetus with coarctation of aorta at 25 weeks of gestation (diagnostic planes with automatic labeling are shown) (also see Videoclip S10). The three-vessels and trachea view shows a narrow transverse aortic arch. In the four-chamber view, the left ventricle appears narrow compared with the right ventricle; however, it is apex-forming. The right side of the heart appears enlarged, and the right ventricle is moderately hypertrophied. The five-chamber view shows a narrow aortic root; there is also a ventricular septal defect (not shown in this frame). The left ventricular outflow tract view also shows a narrow aorta (the ventricular septal defect is not shown in this frame). In the short-axis view of great vessels/right ventricular outflow tract, the cross-section of the aorta is small compared to the pulmonary artery. The abdomen, ductal arch and venae cavae views are normal. In the aortic arch view, the coarctation is demonstrated as narrowing in the isthmus region. A, transverse aortic arch; Ao, aorta; Desc., descending; IVC, inferior vena cava; LA, left atrium; LV, left ventricle; P, pulmonary artery; PA, pulmonary artery; RA, right atrium; RV, right ventricle; RVOT, right ventricular outflow tract; S, superior vena cava; Stom., stomach; SVC, superior vena cava; Tr., transverse; Vent., ventricular.

the pulmonary artery (confirmed via its bifurcation) appears to the right of the aorta on the screen.

Pulmonary atresia with intact ventricular septum

In a fetus with pulmonary atresia and an intact ventricular septum at 29 weeks of gestation, six echocardiography views are abnormal and pulmonary atresia is directly demonstrated in three views (Figure 6, Videoclip S14). The 3VT view shows hypoplasia of the pulmonary artery. In the four-chamber view, the right ventricle appears small, the right atrium is dilated (secondary to tricuspid regurgitation), and a secundum atrial septal defect is present. By activating VIS-Assistance®, it is evident that the right ventricle is truly small. The five-chamber view also shows a small right ventricle and a dilated right

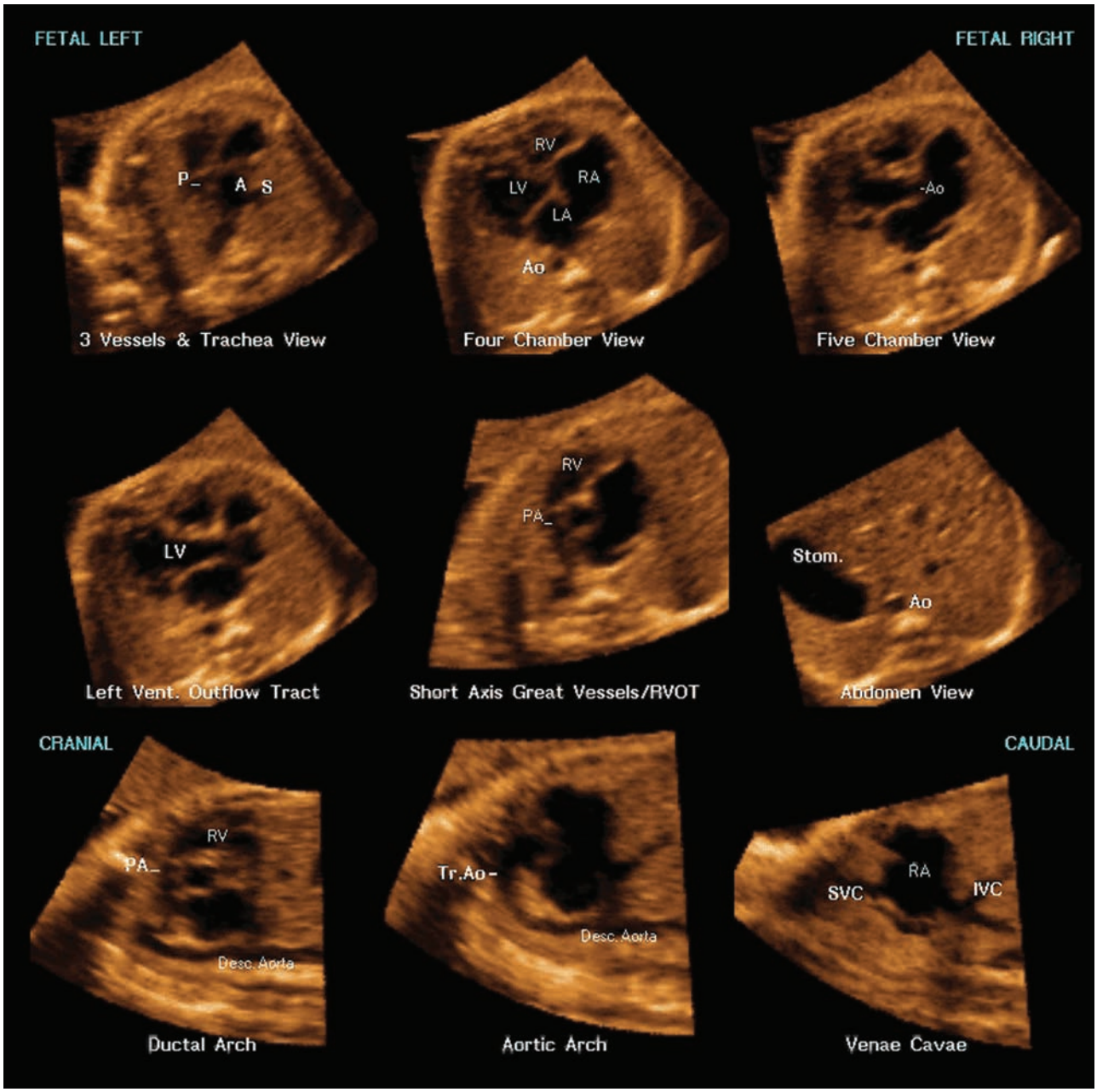

Figure 6 Application of the Fetal Intelligent Navigation Echocardiography (FINE) method to a fetus with pulmonary atresia and an intact ventricular septum at 29 weeks of gestation (diagnostic planes with automatic labeling are shown) (also see Videoclip S14). Six echocardiography views are abnormal, and pulmonary atresia is directly demonstrated in three views. The three-vessels and trachea view shows hypoplasia of the pulmonary artery. In the four-chamber view, the right ventricle appears small, the right atrium is dilated (secondary to tricuspid regurgitation), and a secundum atrial septal defect is present. By activating Virtual Intelligent Sonographer Assistance (VIS-Assistance®; not shown), it is evident that the right ventricle is truly small. The five-chamber view also shows a small right ventricle and a dilated right atrium. In the left ventricular outflow tract view, the aorta appears dilated. The short-axis view of great vessels/right ventricular outflow tract shows hypoplasia of the pulmonary artery and a dilated right atrium. The abdomen, aortic arch and venae cavae views are normal. The ductal arch view also shows hypoplasia of the pulmonary artery, along with a tortuous ductus arteriosus connecting to the descending aorta. A, transverse aortic arch; Ao, aorta; Desc., descending; IVC, inferior vena cava; LA, left atrium; LV, left ventricle; P, pulmonary artery; PA, pulmonary artery; RA, right atrium; RV, right ventricle; RVOT, right ventricular outflow tract; S, superior vena cava; Stom., stomach; SVC, superior vena cava; Tr., transverse; Vent., ventricular.

atrium. In the left ventricular outflow tract view, the aorta appears dilated. The short-axis view of great vessels/right ventricular outflow tract clearly shows hypoplasia of the pulmonary artery and a dilated right atrium. The ductal arch view also shows hypoplasia of the pulmonary artery, along with a tortuous ductus arteriosus connecting to the descending aorta.

DISCUSSION

The conventional method for analysis of a cardiac volume dataset is 'manual navigation'[93] using controls to interrogate the three orthogonal planes in the multiplanar display mode. This is intended to generate a set of standard cardiac views required for prenatal diagnosis.

Unfortunately, many operators examine the fetal heart in this manner without using a systematic approach. Identification of appropriate diagnostic planes is highly operator-dependent, challenging, and is often time-consuming. To address this issue, algorithms have been developed to examine cardiac volume datasets, so that diagnostic planes can be retrieved systematically and efficiently[84–90]. In an important step forward, Abuhamad *et al.* determined, for the first time, the spatial relationship of diagnostic planes of the fetal heart to a reference plane (four-chamber view) within 3D volumes[96]. The same authors then prospectively evaluated the performance of software to automatically retrieve diagnostic fetal cardiac planes from 3D volumes of the chest[91]. Recently, others have reported semi-automated algorithms using xMatrix transducers to display standard echocardiographic views successfully[97].

We report herein a novel and automatic method to visualize nine standard fetal echocardiography views by applying intelligent navigation technology to STIC volume datasets. Indeed, seven of the views have been recommended by the American Institute of Ultrasound in Medicine (AIUM) for performing fetal echocardiography[92]. We also decided to generate the five-chamber view (as reported by others[91,98,99]), along with the fetal stomach[91] (for determination of situs). Marking anatomical structures in different planes of the heart using intelligent navigation allows inferences of the anatomical relationships in multiple dimensions and thus, a geometrical reconstruction of the heart is possible. As a result, the successful display of cardiac diagnostic planes occurs despite different gestational ages, and also in the presence of anatomical variability (e.g. cardiac axis and geometry).

The FINE method is different from our previous algorithms based on STIC[84,86,87,88] because it substantially decreases the number of steps required to obtain echocardiography views, making it less operator-dependent and considerably simplifies examination of the fetal heart. The user is only required to mark anatomical structures of the heart within the volume dataset, which triggers intelligent navigation and results in the display of nine echocardiography views through diagnostic planes/VIS-Assistance®. Our approach is also fundamentally different from other techniques to obtain cardiac views since: 1) it may be used across different gestational ages and its use is not confined to the second trimester; 2) it does not apply to 3D static volumes of the fetal heart; 3) it does not depend on 'fitting' the heart into a predetermined template as an initial step to display cardiac views; 4) manual standardization or manipulation of the STIC volume dataset and reference planes is not required (e.g. alignment or rotation); 5) there is no dependency on tomographic ultrasound imaging (TUI) (which displays multiple images that are parallel and equidistant to each other); 6) it incorporates cardiac phase recognition technology; 7) there is automatic labeling of echocardiography views (i.e. diagnostic planes), anatomical structures, left and right side of the fetus, and cranial and caudal ends; and 8) operator-independent sonographic navigation and exploration of surrounding structures in previously identified diagnostic planes is available (VIS-Assistance®). Table 4 describes further characteristics of the FINE method.

Acquiring an appropriate STIC volume is a requirement for its successful display and analysis[100]. Factors that interfere with image quality in conventional 2D sonography (e.g. fetal positioning, maternal body habitus)[26] will also affect STIC quality[100]. It is important to stress that the FINE method may not be successful in generating fetal echocardiography views if: 1) the quality of the STIC volume dataset is inadequate (e.g. motion artifact); 2) the volume does not contain information about the echocardiography view(s) (e.g. a narrow angle of acquisition resulting in a volume not containing the upper mediastinum and stomach); 3) the STIC volume is not acquired from a true four-chamber view (e.g. a true cross-section of the thorax, proper alignment in the axial plane); 4) the user does not mark the anatomical structures appropriately (e.g. poor visualization or lack of familiarity with anatomy); and 5) a congenital heart defect is present. For example, if the fetal spine is not located between 5 and 7 o'clock within the STIC volume, acoustic shadowing from the ribs or spine may be increased, and visualization rates for fetal echocardiography views using the FINE method are expected to be lower than those reported herein. Therefore, proper acquisition of STIC volume datasets is essential in order to perform the FINE method, and we propose the use of STICLoop™ as an aid in determining the appropriateness of such volumes. Moreover, we wish to emphasize that not all patients and their fetuses are candidates for implementation of the FINE method. Protocols that include the acquisition of more than one volume increase the chances that relevant information can be obtained[101]. Thus, additional STIC acquisitions should be obtained (when possible) if the initial volumes are not appropriate. Since an optimal fetal position can change during the course of a sonographic examination, it is advisable to acquire several STIC volumes when the fetal position is optimal and to continue with live 2D sonography. If the latter is unsuccessful in obtaining cardiac views, the volume datasets are available for analysis.

We propose using the FINE method as an aid for examination of the fetal heart in the population at large, rather than to diagnose specific congenital heart defects. Yet, in a limited number of cases of proven congenital heart defects, the FINE method was able to demonstrate evidence of abnormal cardiac anatomy in all instances. Moreover, this was evident in multiple echocardiography views for each case. We were particularly interested in evaluating fetuses in which the specific abnormality was not apparent in the axial plane (e.g. coarctation of aorta, a difficult diagnosis to make prenatally[102]). For this case, the aortic arch view successfully demonstrated the coarctation in both the diagnostic plane and VIS-Assistance®. In general, the *simultaneous* display of multiple cardiac diagnostic planes was also informative and useful, because: 1) various features of the congenital heart defect could be visualized and compared side by side (e.g. overriding aorta, ventricular septal defect, and

Table 4 Characteristics of Fetal Intelligent Navigation Echocardiography (FINE) used to generate standard fetal echocardiography views

Characteristic	*FINE*
1. Gestational age	Second to third trimesters
2. Ultrasound modality	Volumetric sonography (STIC datasets)
3. Fetal echocardiography views	Nine views: Four chamber Five chamber Left ventricular outflow tract Short-axis view of great vessels/right ventricular outflow tract Three vessels and trachea Abdomen/stomach Ductal arch Aortic arch Superior and inferior vena cava
4. General characteristics	Intelligent navigation (*vs* manual)[93] Seven anatomical structures of fetal heart are marked using Anatomic Box® to generate a geometrical model of the heart (i.e. parsimonious) System automatically and immediately rotates, aligns, dissects and scales volume dataset to display nine cardiac diagnostic planes simultaneously[93] Automatic realignment of STIC volume, and reorientation and standardization of the anatomical position so that the fetus and diagnostic planes are consistently displayed in the same manner each time Method is *predictable* (i.e. diagnostic planes are generated in a consistent way) and *adaptive* ('fits' the anatomy of each particular case under examination) VIS-Assistance® is available for each diagnostic plane
5. Cardiac diagnostic planes	Successful display occurs despite different gestational ages and also in the presence of anatomical variability (e.g. cardiac axis and geometry) All nine planes are displayed simultaneously in a single template
6. VIS-Assistance®	Operator-independent sonographic navigation and exploration of surrounding structures in a cardiac diagnostic plane of interest ('virtual' sonographer)
7. Labeling	Automatic (fetal echocardiography views, anatomical structures, left and right side of fetus, and cranial and caudal ends) Labeling stays with the corresponding anatomical structure(s), even as the image is increased in size (zoom)
8. Cardiac phase recognition	Facilitates marking of anatomical structures (e.g. closed pulmonary valve) and is an important feature to increase the success of obtaining echocardiography views
9. Other characteristics	STICLoop™ (evaluation of STIC volume to determine its appropriateness before applying the FINE method)
10. Technical aspects	Can operate on conventional computers; is not dependent on specific ultrasound platforms or on the use of software to perform manual navigation of volume datasets[93]
11. Telemedicine	STIC volume datasets, diagnostic planes, and VIS-Assistance® videoclips can be transmitted Smartphones, tablets and other devices may also be used to receive the transmitted information (diagnostic planes or VIS-Assistance® videoclips)[93]

STIC, spatiotemporal image correlation; VIS-Assistance®, Virtual Intelligent Sonographer Assistance.

pulmonary stenosis in the case of tetralogy of Fallot); and 2) the same specific abnormality could be confirmed in multiple views at the same time (e.g. hypoplasia of the pulmonary artery visualized in three views: 3VT, short-axis view of great vessels/right ventricular outflow tract, and ductal arch). For some cases, VIS-Assistance® also provided additional information that was not evident in the diagnostic plane. For example, in the case of tetralogy of Fallot, a large ventricular septal defect could be seen in the four-chamber view VIS-Assistance®; however, the diagnostic plane appeared normal. In the fetus with transposition of the great vessels, the five-chamber view diagnostic plane appeared normal. Yet, VIS-Assistance® demonstrated the great vessels arising parallel and side-by-side from the ventricles.

We acknowledge that for other types of congenital heart defects, the FINE method may not be useful or applicable. Examples include: 1) when an abnormality is already obvious in the four-chamber view (e.g. hypoplastic left heart, atrioventricular canal defect); and 2) anatomical structures are not present for marking or in their usual location (e.g. truncus arteriosus). Indeed, if anatomical structures of the fetal heart cannot be successfully marked, this may have several explanations: 1) suboptimal STIC quality (e.g. poor visualization, noninformative volume); 2) lack of familiarity with anatomy; or 3) the presence of congenital heart disease. In such cases, patients should undergo real-time sonographic examination of the fetal heart, and referral to an expert should be considered.

The limitations of intelligent navigation have been described elsewhere[93]. Application of this technology and the FINE method are not intended to replace the performance of real-time fetal echocardiography, in which only the latter can evaluate cardiac function, cardiac rate or rhythm disturbances, Doppler velocimetry, etc. at the present time. For the development and testing phases of the study, the authors determined the success rate of obtaining nine fetal echocardiography views using diagnostic planes and/or VIS-Assistance®. We recognize the possibility that when operators with a different level of experience use the FINE method, visualization rates for fetal echocardiography views may be lower than those

reported herein. This may be a result of the frequency with which appropriate STIC datasets are obtained, the appropriate marking of anatomical structures, familiarity with cardiac anatomy, and therefore, limited assessment and interpretation of echocardiography views.

One strategy to improve the prenatal detection of congenital heart defects is the use of volumetric sonography and Internet consultation[72,101,103,104], in which standard fetal echocardiography views can be obtained from STIC volumes[72,105,106]. A valid concern is that a user may be able to acquire a STIC volume and mark the anatomical structures, but may not have the expertise to read and interpret the resulting images using diagnostic planes and/or VIS-Assistance®. For this user, visualization rates for fetal echocardiography views may be lower than what we have reported. However, as STIC volume datasets, diagnostic planes, and videoclips can be transmitted by telemedicine, expert consultants can evaluate these images.

CONCLUSION

The introduction of novel methods, such as the one proposed herein, may simplify examination of the fetal heart and reduce operator dependency. Moreover, it has the potential of improving the efficiency and workflow of performing fetal echocardiography by reducing the time necessary to obtain standard cardiac views. Through telemedicine, the transmission of information and the ability to obtain expert consultation is facilitated. Using the FINE method, the observation of abnormal echocardiography views in the diagnostic planes and/or VIS-Assistance® should raise the index of suspicion for congenital heart disease.

ACKNOWLEDGMENTS

This work was made possible by a partnership with two unique and outstanding computer scientists, Mr Gustavo Abella and Mr Ricardo Gayoso. The conceptual development, execution, testing, and deployment of FINE represent a concerted effort of years of collaborative work among the authors, Mr Abella and Mr Gayoso. A provisional application for a patent ('Apparatus and Method for Fetal Intelligent Navigation Echocardiography') has been filed through the U.S. Patent and Trademark Office; Dr Lami Yeo, Dr Roberto Romero, Mr Gustavo Abella, and Mr Ricardo Gayoso are co-inventors.

The work of Dr Roberto Romero was supported by the Perinatology Research Branch, Division of Intramural Research, *Eunice Kennedy Shriver* National Institute of Child Health and Human Development, NIH, DHHS. Dr Roberto Romero has contributed to this work as part of his official duties as an employee of the United States Federal Government. Dr Lami Yeo was funded by Wayne State University through a service contract in support of the Perinatology Research Branch. The contributions of Mr Abella and Mr Gayoso were funded by Medge Platforms, Inc., New York, NY, USA.

This research was supported, in part, by the Perinatology Research Branch, Division of Intramural Research, *Eunice Kennedy Shriver* National Institute of Child Health and Human Development, National Institutes of Health, Department of Health and Human Services (NICHD/NIH); and, in part, with Federal funds from NICHD, NIH under Contract No. HHSN275201300006C.

REFERENCES

1. Centers for Disease Control and Prevention (CDC). Improved national prevalence estimates for 18 selected major birth defects: United States 1999-2001. *MMWR Morb Mortal Wkly Rep* 2006; **54**: 1301–1305.
2. Acherman RJ, Evans WN, Luna CF, Rollins R, Kip KT, Collazos JC, Restrepo H, Adasheck J, Iriye BK, Roberts D, Sacks AJ. Prenatal detection of congenital heart disease in southern Nevada: the need for universal fetal cardiac evaluation. *J Ultrasound Med* 2007; **26**: 1715–1719.
3. Achiron R, Glaser J, Gelernter I, Hegesh J, Yagel S. Extended fetal echocardiographic examination for detecting cardiac malformations in low-risk pregnancies. *BMJ* 1992; **304**: 671–674.
4. Robinson JN, Simpson LL, Abuhamad AZ. Screening for fetal heart disease with ultrasound. *Clin Obstet Gynecol* 2003; **46**: 890–896.
5. Smythe JF, Copel JA, Kleinman CS. Outcome of prenatally detected cardiac malformations. *Am J Cardiol* 1992; **69**: 1471–1474.
6. Gembruch U. Prenatal diagnosis of congenital heart disease. *Prenat Diagn* 1997; **17**: 1283–1298.
7. Garne E, Stoll C, Clementi M. Evaluation of prenatal diagnosis of congenital heart diseases by ultrasound: experience from 20 European registries. *Ultrasound Obstet Gynecol* 2001; **17**: 386–391.
8. Westin M, Saltvedt S, Bergman G, Kublickas M, Almstrom H, Grunewald C, Valentin L. Routine ultrasound examination at 12 or 18 gestational weeks for prenatal detection of major congenital heart malformations? A randomized controlled trial comprising 36,299 fetuses. *BJOG* 2006; **113**: 675–682.
9. Nikkila A, Bjorkhem G, Kallen B. Prenatal diagnosis of congenital heart defects—a population based study. *Acta Paediatr* 2007; **96**: 49–52.
10. Friedberg MK, Silverman NH, Moon-Grady AJ, Tong E, Nourse J, Sorenson B, Lee J, Hornberger LK. Prenatal detection of congenital heart disease. *J Pediatr* 2009; **155**: 26–31.
11. Pinto NM, Keenan HT, Minich LL, Puchalski MD, Heywood M, Botto LD. Barriers to prenatal detection of congenital heart disease: a population based study. *Ultrasound Obstet Gynecol* 2012; **40**: 418–425.
12. McBrien A, Sands A, Craig B, Dornan J, Casey F. Major congenital heart disease: antenatal detection, patient characteristics and outcomes. *J Matern Fetal Neonatal Med* 2009; **22**: 101–105.
13. Jaeggi ET, Sholler GF, Jones OD, Cooper SG. Comparative analysis of pattern, management and outcome of pre- versus postnatally diagnosed major congenital heart disease: a population-based study. *Ultrasound Obstet Gynecol* 2001; **17**: 380–385.
14. Sklansky MS, Berman DP, Pruetz JD, Chang RK. Prenatal screening for major congenital heart disease: superiority of outflow tracts over the 4-chamber view. *J Ultrasound Med* 2009; **28**: 889–899.
15. Tibballs J, Cantwell-Barti A. Outcomes of management decisions by parents for their infants with hypoplastic left heart syndrome born with and without a prenatal diagnosis. *J Paediatr Child Health* 2008; **44**: 321–324.

16. Daubeney PE, Sharland GK, Cook AC, Keeton BR, Anderson RH, Webber SA. Pulmonary atresia with intact ventricular septum: impact of fetal echocardiography on incidence at birth and postnatal outcome. UK and Eire Collaborative Study of Pulmonary Atresia with Intact Ventricular Septum. *Circulation* 1998; **98**: 562–566.
17. Franklin O, Burch M, Manning N, Sleeman K, Gould S, Archer N. Prenatal diagnosis of coarctation of the aorta improves survival and reduces morbidity. *Heart* 2002; **87**: 67–69.
18. Schultz AH, Localio AR, Clark BJ, Ravishankar C, Videon N, Kimmel SE. Epidemiologic features of the presentation of critical congenital heart disease: implications for screening. *Pediatrics* 2008; **121**: 751–757.
19. Brown KL, Ridout DA, Hoskote A, Verhulst L, Ricci M, Bull C. Delayed diagnosis of congenital heart disease worsens preoperative condition and outcome of surgery in neonates. *Heart* 2006; **92**: 1298–1302.
20. Tworetzky W, McElhinney DB, Reddy VM, Brook MM, Hanley FL, Silverman NH. Improved surgical outcome after fetal diagnosis of hypoplastic left heart syndrome. *Circulation* 2001; **103**: 1269–1273.
21. Verheijen PM, Lisowski LA, Stoutenbeek P, Hitchcock JF, Bennink GK, Meijboom EJ. Lactacidosis in the neonate is minimized by prenatal detection of congenital heart disease. *Ultrasound Obstet Gynecol* 2002; **19**: 552–555.
22. Kumar RK, Newburger JW, Gauvreau K, Kamenir SA, Hornberger LK. Comparison of outcome when hypoplastic left heart syndrome and transposition of the great arteries are diagnosed prenatally versus when diagnosis of these two conditions is made only postnatally. *Am J Cardiol* 1999; **83**: 1649–1653.
23. Mahle WT, Clancy RR, McGaurn SP, Goin JE, Clark BJ. Impact of prenatal diagnosis on survival and early neurologic morbidity in neonates with the hypoplastic left heart syndrome. *Pediatrics* 2001; **107**: 1277–1282.
24. Bonnet D, Coltri A, Butera G, Fermont L, Le Bidois J, Kachaner J, Sidi D. Detection of transposition of the great arteries in fetuses reduces neonatal morbidity and mortality. *Circulation* 1999; **99**: 916–918.
25. Khoshnood B, De Vigan C, Vodovar V, Goujard J, Lhomme A, Bonnet D, Goffinet F. Trends in prenatal diagnosis, pregnancy termination, and perinatal mortality of newborns with congenital heart disease in France, 1983-2000: a population-based evaluation. *Pediatrics* 2005; **115**: 95–101.
26. DeVore GR, Medearis AL, Bear MB, Horenstein J, Platt LD. Fetal echocardiography: factors that influence imaging of the fetal heart during the second trimester of pregnancy. *J Ultrasound Med* 1993; **12**: 659–663.
27. Hunter S, Heads A, Wyllie J, Robson S. Prenatal diagnosis of congenital heart disease in the northern region of England: benefits of a training programme for obstetric ultrasonographers. *Heart* 2000; **84**: 294–298.
28. Tegnander E, Eik-Nes SH. The examiner's ultrasound experience has a significant impact on the detection rate of congenital heart defects at the second-trimester fetal examination. *Ultrasound Obstet Gynecol* 2004; **24**: 217.
29. International Society of Ultrasound in Obstetrics and Gynecology Guidelines. Cardiac screening examination of the fetus: guidelines for performing the ''basic'' and ''extended basic'' cardiac scans. *Ultrasound Obstet Gynecol* 2006; **27**: 107–113.
30. Allan L. Technique of fetal echocardiography. *Pediatr Cardiol* 2004; **25**: 223–233.
31. Benacerraf BR. Sonographic detection of fetal anomalies of the aortic and pulmonary arteries: value of four-chamber view vs. direct images. *AJR Am J Roentgenol* 1994; **163**: 1483–1489.
32. Carvalho JS, Mavrides E, Shinebourne EA, Campbell S, Thilaganathan B. Improving the effectiveness of routine prenatal screening for major congenital heart defects. *Heart* 2002; **88**: 387–391.
33. Chaoui R. The examination of the normal fetal heart using two-dimensional fetal echocardiography. In *Fetal Cardiology*, Yagel S, Silverman NH, Gembruch U (eds). Martin Dunitz: London, 2003; 141–149.
34. Bromley B, Estroff JA, Sanders SP, Parad R, Roberts D, Frigoletto FD Jr, Benacerraf BR. Fetal echocardiography: accuracy and limitations in a population at high and low risk for heart defects. *Am J Obstet Gynecol* 1992; **166**: 1473–1481.
35. Comstock CH. What to expect from routine midtrimester screening for congenital heart disease. *Semin Perinatol* 2000; **24**: 331–342.
36. Nelson TR, Pretorius DH, Sklansky M, Hagen-Ansert S. Three-dimensional echocardiographic evaluation of fetal heart anatomy and function: acquisition, analysis, and display. *J Ultrasound Med* 1996; **15**: 1–9.
37. Zosmer N, Jurkovic D, Jauniaux E, Gruboeck K, Lees C, Campbell S. Selection and identification of standard cardiac views from three-dimensional volume scans of the fetal thorax. *J Ultrasound Med* 1996; **15**: 25–32.
38. Chang FM, Hsu KF, Ko HC, Yao BL, Chang CH, Yu CH, Liang RI, Chen HY. Fetal heart volume assessment by three-dimensional ultrasound. *Ultrasound Obstet Gynecol* 1997; **9**: 42–48.
39. Sklansky MS, Nelson T, Strachan M, Pretorius DH. Real-time three-dimensional fetal echocardiography: initial feasibility study. *J Ultrasound Med* 1999; **18**: 745–752.
40. Guerra FA, Isla AI, Aguilar RC, Fritz EG. Use of free-hand three-dimensional ultrasound software in the study of the fetal heart. *Ultrasound Obstet Gynecol* 2000; **16**: 329–334.
41. Levi S, Cos-Sanchez T. Fetal echocardiography volume mode (3 dimensions) [in French]. *J Gynecol Obstet Biol Reprod (Paris)* 2000; **29**: 261–263.
42. Scharf A, Geka F, Steinborn A, Frey H, Schlemmer A, Sohn C. 3D real-time imaging of the fetal heart. *Fetal Diagn Ther* 2000; **15**:267–274.
43. Bega G, Kuhlman K. Lev-Toaff A, Kurtz A, Wapner R. Application of three-dimensional ultrasonography in the evaluation of the fetal heart. *J Ultrasound Med* 2001; **20**; 307–313.
44. Michailidis GD, Simpson JM, Karidas C, Economides DL. Detailed three- dimensional fetal echocardiography facilitated by an internet link. *Ultrasound Obstet Gynecol* 2001; **18**: 325–328.
45. Arzt W, Tulzer G, Aigner M. Real time 3D sonography of the normal fetal heart: clinical evaluation [in German]. *Ultraschall Med* 2002; **23**: 388–391.
46. Deng J, Yates R, Sullivan ID, McDonald D, Linney AD, Lees WR, Anderson RH, Rodeck CH. Dynamic three-dimensional color Doppler ultrasound of human fetal intracardiac flow. *Ultrasound Obstet Gynecol* 2002; **20**: 131–136.
47. Maulik D, Nanda NC, Singh V, Dod H, Vengala S, Sinha A, Sidhu MS, Khanna D, Lysikiewicz A, Sicuranza G, Modh N. Live three-dimensional echocardiography of the human fetus. *Echocardiography* 2003; **20**: 715–721.
48. Herberg U, Goldberg H, Breuer J. Three- and four-dimensional freehand fetal echocardiography: a feasibility study using a hand-held Doppler probe for cardiac gating. *Ultrasound Obstet Gynecol* 2005; **25**: 362–371.
49. Espinoza J, Goncalves LF, Lee W, Chaiworapongsa T, Treadwell MC, Stites S, Schoen ML, Mazor M, Romero R. The use of the minimum projection mode in 4-dimensional examination of the fetal heart with spatiotemporal image correlation. *J Ultrasound Med* 2004; **23**: 1337–1348.
50. Goncalves LF, Espinoza J, Lee W, Mazor M, Romero R. Three- and four- dimensional reconstruction of the aortic and ductal arches using inversion mode: a new rendering algorithm for visualization of fluid-filled anatomical structures. *Ultrasound Obstet Gynecol* 2004; **24**: 696–698.
51. DeVore GR, Falkensammer P, Sklansky MS, Platt LD. Spatio-temporal image correlation (STIC): new technology

for evaluation of the fetal heart. *Ultrasound Obstet Gynecol* 2003; **22**: 380–387.
52. Bhat AH, Corbett VN, Liu R, Carpenter ND, Liu NW, Wu AM, Hopkins GD, Li X, Sahn DJ. Validation of volume and mass assessments for human fetal heart imaging by 4-dimensional spatiotemporal image correlation echocardiography: in vitro balloon model experiments. *J Ultrasound Med* 2004; **23**: 1151–1159.
53. Chaoui R, Hoffmann J, Heling KS. Three-dimensional (3D) and 4D color Doppler fetal echocardiography using spatiotemporal image correlation (STIC). *Ultrasound Obstet Gynecol* 2004; **23**: 535–545.
54. Yagel S, Cohen SM, Shapiro I, Valsky DV. 3D and 4D ultrasound in fetal cardiac scanning: a new look at the fetal heart. *Ultrasound Obstet Gynecol* 2007; **29**: 81–95.
55. Turan S, Turan OM, Ty-Torredes K, Harman CR, Baschat AA. Standardization of the first-trimester fetal cardiac examination using spatiotemporal image correlation with tomographic ultrasound and color Doppler imaging. *Ultrasound Obstet Gynecol* 2009; **33**: 652–656.
56. Messing B, Cohen SM, Valsky DV, Shen O, Rosenak D, Lipschuetz M, Yagel S. Fetal heart ventricular mass obtained by STIC acquisition combined with inversion mode and VOCAL. *Ultrasound Obstet Gynecol* 2011; **38**: 191–197.
57. Luewan S, Yanase Y, Tongprasert F, Srisupundit K, Tongsong T. Fetal cardiac dimensions at 14–40 weeks' gestation obtained using cardio-STIC-M. *Ultrasound Obstet Gynecol* 2011; **37**: 416–422.
58. Hamill N, Romero R, Hassan SS, Lee W, Myers SA, Mittal P, Kusanovic JP, Chaiworapongsa T, Vaisbuch E, Espinoza J, Gotsch F, Carletti A, Goncalves LF, Yeo L. Repeatability and reproducibility of fetal cardiac ventricular volume calculations using spatiotemporal image correlation and virtual organ computer- aided analysis. *J Ultrasound Med* 2009; **28**: 1301–1311.
59. Tutschek B, Sahn DJ. Semi-automatic segmentation of fetal cardiac cavities: progress towards an automated fetal echocardiogram. *Ultrasound Obstet Gynecol* 2008; **32**: 176–180.
60. Goncalves LF, Espinoza J, Romero R, Kusanovic JP, Swope B, Nien JK, Erez O, Soto E, Treadwell MC. Four-dimensional ultrasonography of the fetal heart using a novel Tomographic Ultrasound Imaging display. *J Perinat Med* 2006; **34**: 39–55.
61. Goncalves LF, Romero R, Espinoza J, Lee W, Treadwell M, Chintala K, Brandl H, Chaiworapongsa T. Four-dimensional ultrasonography of the fetal heart using color Doppler spatiotemporal image correlation. *J Ultrasound Med* 2004; **23**: 473–481.
62. Wang N, Xie HN, Peng R, Zheng J, Zhu YX. Accuracy, agreement, and reliability of fetal cardiac measurements using 4-dimensional spatiotemporal image correlation. *J Ultrasound Med* 2012; **31**: 1719–1726.
63. Cohen L, Mangers K, Grobman WA, Platt LD. Satisfactory visualization rates of standard cardiac views at 18 to 22 weeks' gestation using spatiotemporal image correlation. *J Ultrasound Med* 2009; **28**: 1645–1650.
64. Hamill N, Yeo L, Romero R, Hassan SS, Myers SA, Mittal P, Kusanovic JP, Balasubramaniam M, Chaiworapongsa T, Vaisbuch E, Espinoza J, Gotsch F, Goncalves LF, Lee W. Fetal cardiac ventricular volume, cardiac output, and ejection fraction determined with 4-dimensional ultrasound using spatiotemporal image correlation and virtual organ computer-aided analysis. *Am J Obstet Gynecol* 2011; **205**: 76.e1–e10.
65. Simioni C, Nardozza LM, Araujo Junior E, Rolo LC, Zamith M, Caetano AC, Moron AF. Heart stroke volume, cardiac output, and ejection fraction in 265 normal fetus in the second half of gestation assessed by 4D ultrasound using spatio-temporal image correlation. *J Matern Fetal Neonatal Med* 2011; **24**: 1159–1167.
66. Molina FS, Faro C, Sotiriadis A, Dagklis T, Nicolaides KH. Heart stroke volume and cardiac output by four-dimensional ultrasound in normal fetuses. *Ultrasound Obstet Gynecol* 2008; **32**: 181–187.
67. Hamill N, Romero R, Hassan S, Lee W, Myers SA, Mittal P, Kusanovic JP, Balasubramaniam M, Chaiworapongsa T, Vaisbuch E, Espinoza J, Gotsch F, Goncalves LF, Mazaki-Tovi S, Erez O, Hernandez-Andrade E, Yeo L. The fetal cardiovascular response to increased placental vascular impedance to flow determined with 4-dimensional ultrasound using spatiotemporal image correlation and virtual organ computer-aided analysis. *Am J Obstet Gynecol* 2013; **208**: 153.e1–e13.
68. Espinoza J, Goncalves LF, Lee W, Mazor M, Romero R. A novel method to improve prenatal diagnosis of abnormal systemic venous connections using three- and four-dimensional ultrasonography and 'inversion mode'. *Ultrasound Obstet Gynecol* 2005; **25**: 428–434.
69. Meyer-Wittkopf M, Cooper S, Vaughan J, Sholler G. Three-dimensional (3D) echocardiographic analysis of congenital heart disease in the fetus: comparison with cross-sectional (2D) fetal echocardiography. *Ultrasound Obstet Gynecol* 2001; **17**: 485–492.
70. Vinals F, Poblete P, Giuliano A. Spatio-temporal image correlation (STIC): a new tool for the prenatal screening of congenital heart defects. *Ultrasound Obstet Gynecol* 2003; **22**: 388–394.
71. Acar P, Dulac Y, Taktak A, Villaceque M. Real time 3D echocardiography in congenital heart disease [in French]. *Arch Mal Coeur Vaiss* 2004; **97**: 472–478.
72. Vinals F, Mandujano L, Vargas G, Giuliano A. Prenatal diagnosis of congenital heart disease using four-dimensional spatio-temporal image correlation (STIC) telemedicine via an Internet link: a pilot study. *Ultrasound Obstet Gynecol* 2005; **25**: 25–31.
73. Paladini D, Sglavo G, Masucci A, Pastore G, Nappi C. Role of four-dimensional ultrasound (spatiotemporal image correlation and sonography-based automated volume count) in prenatal assessment of atrial morphology in cardiosplenic syndromes. *Ultrasound Obstet Gynecol* 2011; **38**: 337–343.
74. Yagel S, Cohen SM, Rosenak D, Messing B, Lipschuetz M, Shen O, Valsky DV. Added value of three-/four-dimensional ultrasound in offline analysis and diagnosis of congenital heart disease. *Ultrasound Obstet Gynecol* 2011; **37**: 432–437.
75. Hata T, Tanaka H, Noguchi J, Dai SY, Yamaguchi M, Yanagihara T. Four-dimensional volume-rendered imaging of the fetal ventricular outflow tracts and great arteries using inversion mode for detection of congenital heart disease. *J Obstet Gynaecol Res* 2010; **36**: 513–518.
76. Volpe P, Tuo G, De Robertis V, Campobasso G, Marasini M, Tempesta A, Gentile M, Rembouskos G. Fetal interrupted aortic arch: 2D-4D echocardiography, associations and outcome. *Ultrasound Obstet Gynecol* 2010; **35**: 302–309.
77. Gindes L, Hegesh J, Weisz B, Gilboa Y, Achiron R. Three and four dimensional ultrasound: a novel method for evaluating fetal cardiac anomalies. *Prenat Diagn* 2009; **29**: 645–653.
78. Shih JC, Shyu MK, Su YN, Chiang YC, Lin CH, Lee CN. 'Big-eyed frog' sign on spatiotemporal image correlation (STIC) in the antenatal diagnosis of transposition of the great arteries. *Ultrasound Obstet Gynecol* 2008; **32**: 762–768.
79. Dan-Dan W, Xiao-Peng D, Wei C, Hui L. The value of spatiotemporal image correlation technique in the diagnosis of fetal ventricular septal defect. *Arch Gynecol Obstet* 2011; **283**: 965–969.
80. Zhang M, Pu DR, Zhou QC, Peng QH, Tian LQ. Four-dimensional echocardiography with B-flow imaging and spatiotemporal image correlation in the assessment of congenital heart defects. *Prenat Diagn* 2010; **30**: 443–448.

81. Ghi T, Cera E, Segata M, Michelacci L, Pilu G, Pelusi G. Inversion mode spatio-temporal image correlation (STIC) echocardiography in three-dimensional rendering of fetal ventricular septal defects. *Ultrasound Obstet Gynecol* 2005; **26**: 679–680.
82. Hongmei W, Ying Z, Ailu C, Wei S. Novel application of four-dimensional sonography with B-flow imaging and spatiotemporal image correlation in the assessment of fetal congenital heart defects. *Echocardiography* 2012; **29**: 614–619.
83. Bennasar M, Martinez JM, Gomez O, Bartrons J, Olivella A, Puerto B, Gratacos E. Accuracy of four-dimensional spatiotemporal image correlation echocardiography in the prenatal diagnosis of congenital heart defects. *Ultrasound Obstet Gynecol* 2010; **36**: 458–464.
84. Goncalves LF, Lee W, Chaiworapongsa T, Espinoza J, Schoen ML, Falkensammer P, Treadwell M, Romero R. Four-dimensional ultrasonography of the fetal heart with spatiotemporal image correlation. *Am J Obstet Gynecol* 2003; **189**: 1792–1802.
85. DeVore GR, Polanco B, Sklansky MS, Platt LD. The 'spin' technique: a new method for examination of the fetal outflow tracts using three-dimensional ultrasound. *Ultrasound Obstet Gynecol* 2004; **24**: 72–82.
86. Espinoza J, Kusanovic JP, Goncalves LF, Nien JK, Hassan S, Lee W, Romero R. A novel algorithm for comprehensive fetal echocardiography using 4-dimensional ultrasonography and tomographic imaging. *J Ultrasound Med* 2006; **25**: 947–956.
87. Yeo L, Romero R, Jodicke C, Kim SK, Gonzalez JM, Ogge G, Lee W, Kusanovic JP, Vaisbuch E, Hassan S. Simple targeted arterial rendering (STAR) technique: a novel and simple method to visualize the fetal cardiac outflow tracts. *Ultrasound Obstet Gynecol* 2011; **37**: 549–556.
88. Yeo L, Romero R, Jodicke C, Ogge G, Lee W, Kusanovic JP, Vaisbuch E, Hassan S. Four-chamber view and 'swing technique' (FAST) echo: a novel and simple algorithm to visualize standard fetal echocardiographic planes. *Ultrasound Obstet Gynecol* 2011; **37**: 423–431.
89. Rizzo G, Capponi A, Muscatello A, Cavicchioni O, Vendola M, Arduini D. Examination of the fetal heart by four-dimensional ultrasound with spatiotemporal image correlation during routine second-trimester examination: the 'three-steps technique'. *Fetal Diagn Ther* 2008; **24**: 126–131.
90. Jantarasaengaram S, Vairojanavong K. Eleven fetal echocardiographic planes using 4-dimensional ultrasound with spatiotemporal image correlation (STIC): a logical approach to fetal heart volume analysis. *Cardiovasc Ultrasound* 2010; **8**: 41.
91. Abuhamad A, Falkensammer P, Reichartseder F, Zhao Y. Automated retrieval of standard diagnostic fetal cardiac ultrasound planes in the second trimester of pregnancy: a prospective evaluation of software. *Ultrasound Obstet Gynecol* 2008; **31**: 30–36.
92. American Institute of Ultrasound in Medicine. AIUM practice guideline for the performance of fetal echocardiography. *J Ultrasound Med* 2011; **30**: 127–136.
93. Yeo L, Romero R. Intelligent navigation to improve obstetrical sonography. *Ultrasound Obstet Gynecol* (in press).
94. Allan LD, Tynan MJ, Campbell S, Wilkinson JL, Anderson RH. Echocardiographic and anatomical correlates in the fetus. *Br Heart J* 1980; **44**: 444–451.
95. Tongsong T, Tongprasert F, Srisupundit K, Luewan S. The complete three-vessel view in prenatal detection of congenital heart defects. *Prenat Diagn* 2010; **30**: 23–29.
96. Abuhamad A, Falkensammer P, Zaho Y. Automated sonography: defining the spatial relationship of standard diagnostic fetal cardiac planes in the second trimester of pregnancy. *J Ultrasound Med* 2007; **26**: 501–507.
97. Espinoza J, Lee W. xMatrix array and mechanical 4-dimensional volume transducers for standardized views of the fetal heart using an automated algorithm. *J Ultrasound Med* 2011; **30**: S63.
98. Yagel S, Cohen SM, Achiron R. Examination of the fetal heart by five short-axis views: a proposed screening method for comprehensive cardiac evaluation. *Ultrasound Obstet Gynecol* 2001; **17**: 367–369.
99. Chaoui R, McEwing R. Three cross-sectional planes for fetal color Doppler echocardiography. *Ultrasound Obstet Gynecol* 2003; **21**: 81–93.
100. Uittenbogaard LB, Haak MC, Spreeuwenberg MD, Van Vugt JM. A systematic analysis of the feasibility of four-dimensional ultrasound imaging using spatiotemporal image correlation in routine fetal echocardiography. *Ultrasound Obstet Gynecol* 2008; **31**: 625–632.
101. Vinals F. Current experience and prospect of internet consultation in fetal cardiac ultrasound. *Fetal Diagn Ther* 2011; **30**: 83–87.
102. Head CE, Jowett VC, Sharland GK, Simpson JM. Timing of presentation and postnatal outcome of infants suspected of having coarctation of the aorta during fetal life. *Heart* 2005; **91**: 1070–1074.
103. Vinals F, Ascenzo R, Naveas R, Huggon I, Giuliano A. Fetal echocardiography at 11 + 0 to 13 + 6 weeks using four-dimensional spatiotemporal image correlation telemedicine via Internet link: a pilot study. *Ultrasound Obstet Gynecol* 2008; **31**: 633–638.
104. Roberts D. How best to improve antenatal detection of congenital heart defects. *Ultrasound Obstet Gynecol* 2008; **32**: 846–848.
105. Espinoza J, Lee W, Comstock C, Romero R, Yeo L, Rizzo G, Paladini D, Vinals F, Achiron R, Gindes L, Abuhamad A, Sinkovskaya E, Russell E, Yagel S. Collaborative study on 4-dimensional echocardiography for the diagnosis of fetal heart defects: the COFEHD study. *J Ultrasound Med* 2011; **29**: 1573–1580.
106. Adriaanse BM, Tromp CH, Simpson JM, Van Mieghem T, Kist WJ, Kuik DJ, Oepkes D, Van Vugt JM, Haak MC. Interobserver agreement in detailed prenatal diagnosis of congenital heart disease by telemedicine using four-dimensional ultrasound with spatiotemporal image correlation. *Ultrasound Obstet Gynecol* 2012; **39**: 203–209.

SUPPORTING INFORMATION ON THE INTERNET

Figures S1–S3 and **Videoclips S1–S14** may be found in the online version of this article.